

Raman Spectroscopy Based On-Line, Real-Time Monitoring to Reduce Composition Uncertainties

Enhanced sensitivity through optimization of Raman Parameters

August 2021

Amanda M Lines
Heather M Felmy
Samuel A Bryan
Michael J Minette

DISCLAIMER

This report was prepared as an account of work sponsored by an agency of the United States Government. Neither the United States Government nor any agency thereof, nor Battelle Memorial Institute, nor any of their employees, **makes any warranty, express or implied, or assumes any legal liability or responsibility for the accuracy, completeness, or usefulness of any information, apparatus, product, or process disclosed, or represents that its use would not infringe privately owned rights.** Reference herein to any specific commercial product, process, or service by trade name, trademark, manufacturer, or otherwise does not necessarily constitute or imply its endorsement, recommendation, or favoring by the United States Government or any agency thereof, or Battelle Memorial Institute. The views and opinions of authors expressed herein do not necessarily state or reflect those of the United States Government or any agency thereof.

PACIFIC NORTHWEST NATIONAL LABORATORY
operated by
BATTELLE
for the
UNITED STATES DEPARTMENT OF ENERGY
under Contract DE-AC05-76RL01830

Printed in the United States of America

Available to DOE and DOE contractors from
the Office of Scientific and Technical
Information,
P.O. Box 62, Oak Ridge, TN 37831-0062
www.osti.gov
ph: (865) 576-8401
fox: (865) 576-5728
email: reports@osti.gov

Available to the public from the National Technical Information Service
5301 Shawnee Rd., Alexandria, VA 22312
ph: (800) 553-NTIS (6847)
or (703) 605-6000
email: info@ntis.gov
Online ordering: <http://www.ntis.gov>

Raman Spectroscopy Based On-Line, Real-Time Monitoring to Reduce Composition Uncertainties

Enhanced sensitivity through optimization of Raman Parameters

August 2021

Amanda M Lines
Heather M Felmy
Samuel A Bryan
Michael J Minette

Prepared for
the U.S. Department of Energy
under Contract DE-AC05-76RL01830

Pacific Northwest National Laboratory
Richland, Washington 99354

Abstract

Optical spectroscopy-based on-line monitoring of Hanford processing streams can enable real-time characterization of chemical composition of process streams and batches, ultimately enabling and enhancing process control. It can provide immediate feedback on process conditions and has the potential to reduce the needed number of grab sample collections, thereby reducing times and costs associated with laboratory processing.

Here we discuss the utilization of Raman spectroscopy to quantify multiple target analytes that are common within Hanford tanks and waste processing streams. Analytes include: nitrate, nitrite, carbonate, chromate, sulfate, phosphate, hydroxide, oxalate, ammonia, and aluminate. Most notably in this work, Raman applications to low-concentration streams are explored and optimized. Raman instrument specifications are compared; specifically, the impact of utilizing three different Raman excitation wavelengths, 405, 532, and 671 nm, is discussed. Also, Raman data collection parameters such as collection time and spectral averaging are measured and discussed.

Finally, optical libraries of chemical targets were collected using optimized collection parameters and chemometric models were built to automate quantification of chemical targets. These models were validated through application to simulants and real Hanford process samples. Chemometric models performed well on both training and validation sets, suggesting these approaches can be successfully applied to on-line and real-time monitoring of low concentration Hanford processing streams.

The use of the combine Raman wave lengths with the enhanced chemometric models for the low concentration streams significantly improved the chemical detection levels and significantly reduced uncertainties of those measurements.

Summary

Optical spectroscopy-based process monitoring approaches are powerful tools for gaining insight into chemical composition information of a given process stream. Optical approaches can provide a range of chemical information, a key example being Raman spectroscopy which was used in this work to identify and quantify molecular species. Specifically, Raman spectroscopy was used in conjunction with chemometric modeling to quantify nitrate, nitrite, carbonate, chromate, sulfate, phosphate, hydroxide, oxalate, ammonia, and aluminate.

Previous demonstrations verify that Raman spectroscopy can be successfully applied to characterization of real Hanford waste streams. However, questions were present regarding whether Raman could be applied to low concentration streams created during the immobilization of the waste. An example being the melter off-gas condensate, where on-line monitoring could potentially help maintain accountancy as streams are recycled back into subsequent process batches. This project sought primarily to address these concerns and enhance Raman limits of detection by optimizing instrument specifications and collection parameters. This included comparing Raman response from three different commercially available Raman systems using a 405 nm (blue), 532 nm (green), and 671 nm (red) laser excitation source. Signal intensity increased with a decreasing excitation wavelength. Also, parameters such as collection time and spectral averaging were optimized to improve system sensitivity. Overall, while the blue system exhibited the highest sensitivity, the green system presented the best compromise between increased sensitivity with limited introduction of the fluorescence background that interfered with the blue measurements. Similarly, increased sensitivity was observed with longer collection times and higher averaging rates but a compromise was required to increase sensitivity without requiring excessive time periods between data outputs.

After identifying optimized collection parameters optical training sets were collected capturing the fingerprints of the 10 target analytes across a concentration range of interest for process streams such as the melter off-gas condensate. These data sets were used to build chemometric models for quantifying targets in real-time. A variety of modeling approaches were explored to maximize model accuracy and efficiency. Comparisons between models built to utilize only one Raman system (red, green, or blue) and models that simultaneously used data from all three systems (multiblock modeling) were completed. While both approaches performed well, the multiblock approach produced the highest accuracy, lowest uncertainty, results.

Models were applied to spectra of simulants and real Hanford waste processing samples obtained from the PNNL Radioactive Waste Test platform. Models performed well, accurately quantifying key targets at low concentrations. Overall, this demonstrates Raman monitoring can be successfully applied to low concentration Hanford streams. This report was completed under the NQAP NQA-1 program at the basic research technology level.

Acknowledgments

This work was funded by the U.S. Department of Energy Office of River Protection (ORP). Thank you to Isabelle Wheeler (ORP) for oversight and support. Thank you to Michael Stone (SRNL) for guidance and input related to the use of alternative inline monitoring systems. An additional thanks to Matt Wilburn for technical editing. The authors are also grateful to John Vienna for technical support and guidance.

Quality Assurance

This work was performed in accordance with the Pacific Northwest National Laboratory (PNNL) Nuclear Quality Assurance Program (NQAP). The NQAP complies with DOE Order 414.1D, Quality Assurance, and 10 CFR 830, Nuclear Safety Management, Subpart A, Quality Assurance Requirements. The NQAP uses NQA-1-2012, Quality Assurance Requirements for Nuclear Facility Application, as its consensus standard and NQA-1-2012, Subpart 4.2.1, as the basis for its graded approach to quality. The NQAP works in conjunction with PNNL's laboratory-level Quality Management Program, which is based on the requirements as defined in DOE Order 414.1D and 10 CFR 830 Subpart A, Quality Assurance Requirements. This work was graded and performed to direct future research activities. Data contained herein should not be used for, or be used to directly support, design input.

Acronyms and Abbreviations

CV	Cross validation
HLW	High level waste
LAW	Low activity waste
LOD	Limit of detection
LWR	Locally weighted regression
PLS	Partial least squares
PNNL	Pacific Northwest National Laboratory
RMSEC	Root mean square error of calibration
RMSECV	Root mean square error of cross validation
RMSEP	Root mean square error of prediction

Contents

Abstract.....	3
Summary.....	4
Acknowledgments.....	5
Quality Assurance.....	6
Acronyms and Abbreviations	7
Contents.....	8
1.0 Introduction	10
2.0 Experimental details.....	13
2.1 Instrument details	13
2.2 Sample set preparation	13
2.3 Chemometric modeling	13
3.0 Optimization of instrument and collection parameters	14
3.1 Comparison of three Raman systems	14
3.2 Optimizing collection parameters	15
3.3 Final notes on optimized parameters and anticipated limits of detection	17
4.0 Collection of training sets and building of chemometric models.....	20
5.0 Application to Hanford tank processing samples and simulants	29
6.0 Next steps for implementation into the Hanford Direct Feed Low Activity Waste processing.....	35
7.0 Conclusions.....	37
8.0 References.....	38

Figures

Figure 1-1. Estimate of the metric tons of the most common constituents of Hanford tanks (left), spectral signatures of common Raman active species present in tanks (right).....	11
Figure 3-1. Picture of samples within the red, green, and blue sample holders, illuminated by the excitation lasers.....	14
Figure 3-2. Raman spectra of 3 M nitrate on the red, green, and blue systems with 100 mW laser power and 0.5 sec integration time. The inset shows the nitrate band.	15
Figure 3-3. Raman spectra of 3 M nitrate (left) and 0.15 M oxalate (right) measured on the 405 nm (top), 532 nm (middle), and 671 nm (bottom) systems as collection time is varied from 1-10 seconds. On all three Raman systems spectral intensity increases with collection time. Note, lasers were set to dissimilar power settings	16
Figure 3-4. Raman spectra of 3 M nitrate (left) and 0.15 M oxalate (right) measured on the 405 nm (top), 532 nm (middle), and 671 nm (bottom) systems as	

averaging rate is varied from 1 to 100. On all three Raman systems the signal to noise ratio improves as averaging rate increases..... 17

Figure 4-1. Examples of spectral signatures (top) and preprocessed spectra (middle) used for single variate calibration curves (bottom) for the sulfate band for the 405 nm system (left) and aluminate band on the 671 nm system (right). 21

Figure 4-2. Parity plots of training set models built for each laser system separately and analyzing analytes separately. These example results include CrO_4^{2-} (A-C), NO_3^- (D-F), $\text{C}_2\text{O}_4^{2-}$ (G-I), and $\text{Al}(\text{OH})_4^-$ (J-L). 26

Figure 4-3. Parity plots of training set models built using multiblock modeling of all 3 laser systems and modeling all analytes separately. 27

Figure 5-1. Raman spectra of real-tank processing samples measured with the 671 nm (left), 532 nm (middle) and 405 nm (right) systems. Each spectrum was measured at 0.1 sec integration time and represents an average of 200 spectra..... 30

Figure 5-2. Preprocessed Raman spectra of real-tank processing samples measured with the 671 nm (left), 532 nm (middle) and 405 nm (right) systems. Preprocessing included: 1st derivative, normalization to the water band, and mean centering. Each spectrum was measured at 0.1 sec integration time and represents an average of 200 spectra. 32

Figure 5-3. Parity plots of training set models overlayed with validation set results built using multiblock modeling of all 3 laser systems together. 33

Tables

Table 2-1. Chemicals used for the training set including chemical origins, details, and concentration ranges used 13

Table 3-1. LOD values for nitrate and oxalate varying laser power, integration time, and spectral averaging for the 405, 532, and 671 nm excitation lasers. Spectral preprocessing included a 1st derivative, normalizing to the water band, followed by mean centering..... 18

Table 4-1. Training set target analytes and concentration ranges..... 20

Table 4-2. LODs for target analytes on the red, green, and blue systems. Spectral preprocessing included a 1st derivative, normalizing to the water band, followed by mean centering..... 22

Table 4-3. Modeling statistics for the models shown in Figure 4-2: RMSECV=uncertainty, M 28

Table 4-4. Modeling statistics for the models shown in Figure 4-3: RMSECV=uncertainty, M 28

Table 5-1. Samples included in the validation set with molar concentrations of each analyte..... 29

Table 5-2. Comparison of known Hanford waste, waste concentrate, and evaporate samples used as analyte validation set concentrations compared to chemometrically measured concentrations. 34

1.0 Introduction

On-line monitoring, or real-time and *in situ* process characterization, is the optimal route to provide comprehensive characterization of process streams to reduce uncertainties surrounding stream composition. Currently, on-line monitoring techniques are used in a variety of industries where they have enabled significant improvements in process control and reductions in process costs, particularly related to sampling (De Beer et al. 2011, De Leersnyder et al. 2018). Numerous tools are available on the market to provide a robust range of process information. Characterization of chemical composition is particularly valuable for chemical process control and verification.

Optical spectroscopy-based monitoring approaches are uniquely suited to providing detailed chemical composition information on a process stream (Bryan et al. 2011, Casella et al. 2015, Nelson et al. 2021, Tse et al. 2020). First and foremost, optical approaches can provide a range of chemical information, enabling identification and quantification of elemental and molecular species within the process stream. In addition to this, optical approaches are generally mature and can be flexibly integrated into a variety of process types (Clifford et al. 2021, Felmy et al. 2021, Schroll et al. 2016). As an example, optical spectroscopy probes can be plumbed into hazardous environments and are robust enough to withstand radiation dose, corrosive media, high temperatures, and wide ranges of pressures. Note, that while probes can be located in hazardous environments, instrumentation and control equipment can be located in distant, safe locations with only fiber optics traversing the space between detectors and probes.

These techniques are highly applicable to low activity waste (LAW) and high level waste (HLW) process streams that need to be monitored within the tank farms to support compliance, corrosion control, and process control. Of particular interest is Raman spectroscopy, which can be used to uniquely identify and quantify numerous tank waste anions (Bryan et al. 2006, Lines et al. 2019, Tse et al. 2020). Figure 1 presents a chart listing the top chemical contributors to Hanford waste by mass, along with the Raman signatures of the nine Raman-active species from that list. Raman spectroscopy methods and equipment are both mature and commercially available. Furthermore, these systems have been assembled into continuous on-line monitoring systems by PNNL to support Hanford single-shell tank retrievals, engineering-scaled tests at PNNL to support waste pretreatment (Bryan et al. 2006), and, more recently, to support nuclear fuel reprocessing (Lines et al. 2019). Raman technology is ideal for applications to on-line monitoring of tank materials because of the simple yet powerful way this form of spectroscopy works. Raman is a fast (~1 to 5 second measurement), nondestructive technique that relies on interrogating a system with an excitation laser and picking up the inelastically backscattered light. An optical window or penetration port is all that is required to allow Raman interrogation of a stream. The Raman probe itself contains only optics and no electronics, which enables it to maintain a long functional lifetime in radiation and chemically harsh environments. All electronics including the laser excitation source, field deployable detector, and computer for analysis can be located at the other end of fiber optic cables, as far away from hazardous environments as needed.

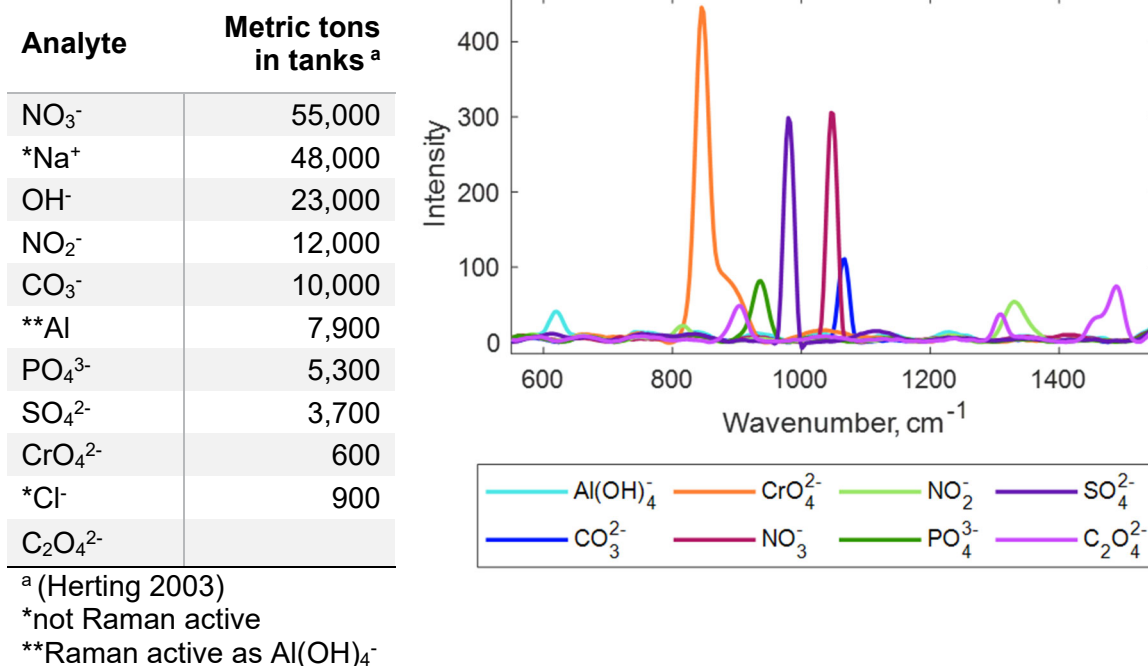


Figure 1-1. Estimate of the metric tons of the most common constituents of Hanford tanks (left), spectral signatures of common Raman active species present in tanks (right)

When combined with chemometric analysis, a form of machine learning, on-line monitoring systems can be developed to analyze spectra and output results in real-time (Felmy et al. 2021, Lines et al. 2020, Lines et al. 2019). This facilitates the transformation of raw data into refined information that can be used by a process operator to easily understand process conditions (Beebe, Pell, and Seasholtz 1998, Bro and Elden 2009, Gallagher et al. 2006). The project team has experience not only in developing these systems, but also working with a small business partner to commercialize the equipment and chemometric models into systems that can be procured commercially and then maintained by the small business (Nelson et al. 2018, Nelson et al. 2019).

The net benefits and alternative options for the proposed future operational sampling regime for the Low-Activity Waste (LAW) Facility, were outlined in previous studies (PNNL-25835 and PNNL-26996). Following issuance of these reports, the collective team agreed that significant potential benefits could be achieved by focusing on process control through a material balance initiative and extending the existing glass algorithms, which was not explicitly specified as part of the original work scope. Targeting key analytes of concern emerged as a secondary area for assessment as part of controlling critical operational parameters within the facility in real time.

Here we discuss efforts to expand applicability of the Raman technique to additional processing streams. Previous demonstrations indicated successful application to real waste samples, e.g. AP-105 solution after filtration and removal of Cs (Lines et al. 2019). However previous demonstrations focused on process streams exhibiting relatively high concentrations of target species. With the goal of applying this approach to low-concentration streams such as melter off-gas condensates, current efforts have focused on optimizing techniques to reduce limits of detection, improve accuracy for measuring low level concentrations, and to reduce measurement

uncertainties. To overcome this challenge, two advancements have been pursued under current work and will be discussed in subsequent sections:

- 1) Optimization of Raman specifications and data collection parameters
- 2) Building of chemometric models that apply multivariate analysis to complex Raman data to extract key concentration information

2.0 Experimental details

2.1 Instrument details

Raman spectrometers were procured from Spectral Solutions, Inc, and utilized thermoelectric-cooled charge-coupled device detectors. Three Raman instruments were used here and equipped with a 671 nm, 532 nm, and 405 nm diode laser respectively. The spectrophotometers' spectral ranges cover approximately 250 cm^{-1} to 4000 cm^{-1} with about 2 cm^{-1} spectral resolution. Integration times and averaging rates were varied and described below. Laser power settings were also varied and described in the following sections.

2.2 Sample set preparation

Initial system optimization was performed on a subset of the full training set. This included the nitrate samples which were expected to have one of the strongest Raman signals and the oxalate samples which have the lowest intensity Raman signature. This subset was used to study the effect of varying integration time, spectra averaging, and excitation laser power to determine the optimal settings for the collection of the full training set.

The entire training set consisted of solutions prepared from the chemicals listed in Table 2-1. For each set of samples in the training set, 10-12 solutions were prepared for each analyte spanning the concentration ranges listed in Table 2-1. $\text{Al}(\text{NO}_3)_3$ and NaAlO_2 solutions were prepared by dissolving the solid in enough excess NaOH to dissolve the aluminum as $\text{Al}(\text{OH})_4^-$. All solutions except the ammonium solutions were prepared with at least 0.1 M excess NaOH to maintain high pH and better simulate the conditions of the actual tank waste samples. Validation set samples included 10 solutions consisting of mixtures of 4 to 9 of the analytes in Table 2-1 in the lower concentration ranges of the training set to test the chemometric model's ability to quantify low concentrations.

Table 2-1. Chemicals used for the training set including chemical origins, details, and concentration ranges used

Analyte	Chemical Details	Concentration, M
NaOH	Ricca, 10.0 N	0.05 - 8
$\text{Al}(\text{NO}_3)_3(\text{H}_2\text{O})_9$	Sigma-Aldrich, $\geq 98\%$	0.001 - 1 M
NaAlO_2	Sigma-Aldrich	0.001 - 1 M
Na_2CO_3	Sigma-Aldrich, $\geq 99.5\%$	0.01 - 2 M
$\text{Na}_2\text{CrO}_4(\text{H}_2\text{O})_4$	Sigma-Aldrich, 99%	0.0005 - 1 M
NaNO_3	Sigma-Aldrich, $\geq 99.0\%$	0.01 - 3 M
NaNO_2	Sigma-Aldrich, $\geq 99.0\%$	0.01 - 1 M
$\text{Na}_3\text{PO}_4(\text{H}_2\text{O})_{12}$	Acros Organics, 98+%	0.0005 - 0.5 M
Na_2SO_4	Sigma-Aldrich, $\geq 99\%$	0.0005 - 0.75 M
$\text{Na}_2\text{C}_2\text{O}_4$	Sigma-Aldrich, $\geq 99.5\%$	0.0005 - 0.15 M
NH_4NO_3	Acros Organics, 99+%	0.005 - 5 M
NH_4OH	J.T. Baker, 5 N	0.5 - 5 M

2.3 Chemometric modeling

Chemometric models were generated using the Eigenvector Research PLS toolbox (version 8.9) for MATLAB (version R2020b). Modeling approaches and details are covered in following sections along with cross validation and figures of merit. Models can be loaded into Spectra Solutions Inc. software SpectraChem to output real-time information in conjunction with spectral collection.

3.0 Optimization of instrument and collection parameters

As discussed in the Introduction, Raman spectroscopy is a particularly valuable optical approach in Hanford processing because it can be used to identify and quantify a significant percentage of tank components. However, given the variety of processing steps between removing liquid waste from tanks and transferring material into its final waste form, a versatile technique that can follow targets across a range of concentrations is needed.

A primary goal of current work is to expand applicability of Raman-based monitoring approaches to waste processing streams exhibiting very low concentrations of target analytes. A key example focused on here is the analysis of melter off-gas streams, particularly focusing on the off-gas evaporate and condensate. Because these streams are recycled back into subsequent melter runs, it is necessary to characterize the chemical constituents (even at their low concentrations) to ensure conditions in the melter and composition of end product are controlled.

Previous demonstrations indicated Raman is a valuable technique for these streams (Lines et al. 2019), however the initial instrument specifications and collection parameters suggested limits of detection (LOD) may not be ideal for analysis of low concentration condensate streams. Here several optimization approaches are considered including utilizing different Raman excitation lasers and modifying collection parameters such as integration time and spectral averaging.

3.1 Comparison of three Raman systems

Three separate Raman systems were evaluated to explore the ability to reduce LODs for key targets of interest to Hanford waste processing schemes. These included Raman systems with 671 nm (red), 532 nm (green), and 405 nm (blue) excitation lasers. Figure 3-1 presents a picture of the three flow cells being excited by the three differently colored laser systems. Previous demonstrations on tank samples utilized a laser system with a 671 nm excitation, however Raman signal is known to increase, thereby improving LODs, with lower wavelength excitation. There is a tradeoff to be wary of in these systems, namely, signal strength may improve with lowering the excitation wavelength but the likelihood of observing interfering fluorescence backgrounds also increases.

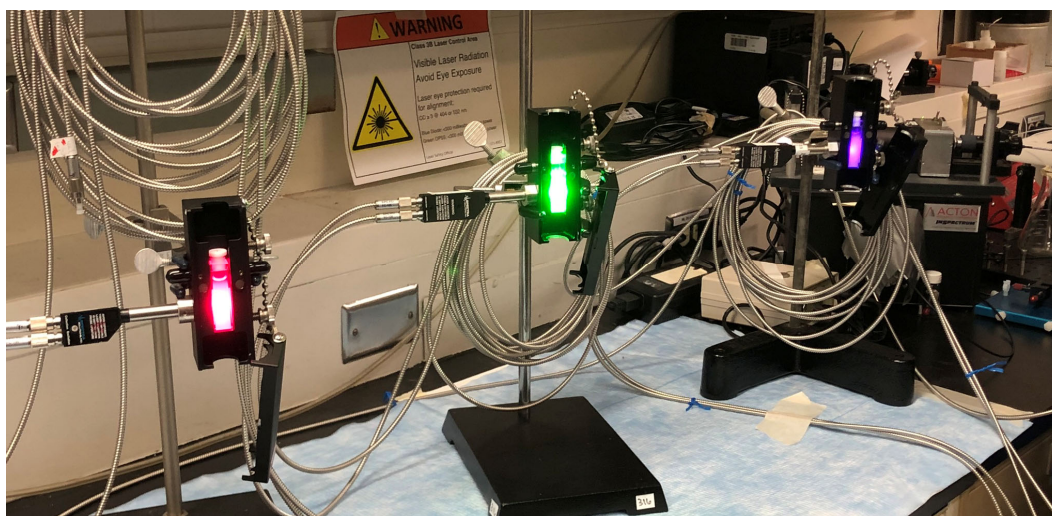


Figure 3-1. Picture of samples within the red, green, and blue sample holders, illuminated by the excitation lasers.

A test set containing samples that could test a range of Raman response were utilized to characterize and optimize instrument specifications and data collection parameters. This set is outlined in the Experimental section (see Table 2-1) and contains samples with very strong (e.g. nitrate) and very weak (e.g. oxalate) Raman fingerprints. An initial comparison of Raman response across the three instruments, where all three lasers were set to ~100 mW power, produced expected results. At similar laser powers, the signal from the blue system was higher than that of the green system, which was higher than that of the red system. Figure 3-2 below provides examples of spectra of a 3 M nitrate sample and demonstrates the significant difference in signal response from the three systems.

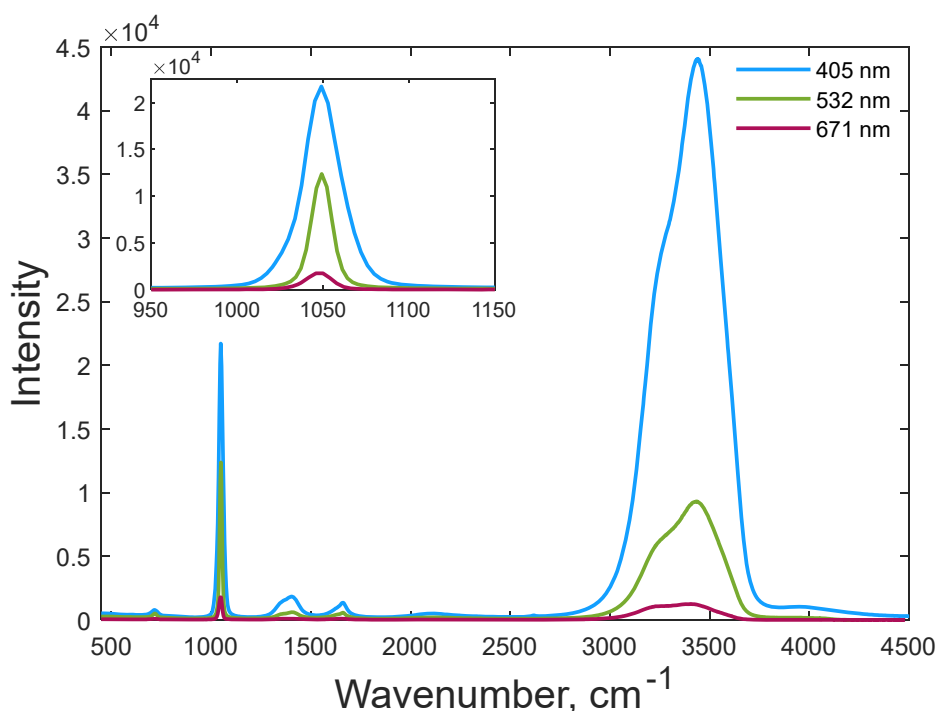


Figure 3-2. Raman spectra of 3 M nitrate on the red, green, and blue systems with 100 mW laser power and 0.5 sec integration time. The inset shows the nitrate band.

Limits of detection followed expected trends, where up to a 15x improvement in LOD for nitrate was observed between the red and blue systems when all systems were at the same ~100 mW power and collection parameters were not further optimized. Table 3-1 lists the calculated limits of detection from the various systems under various collection parameters and section 3.3 provides a collated overview of the best system specifications for analysis of low concentration waste samples.

3.2 Optimizing collection parameters

In addition to varying excitation laser wavelength, varying collection parameters such as integration time or spectral averaging can improve measured signal to noise. Collection time describes the length of time the detector collects photons, where increasing collection time correlates to collecting more photons, increasing observed signal. Spectral averaging describes the number of spectra collected and averaged into a single spectrum before using the “final” resulting spectra for analysis. Increasing the number of averaged spectra improves signal to noise

ratio. From this it is clear that LODs can be improved by increasing either collection time or the number of spectra averaged. However, similar to reducing excitation wavelength, there are tradeoffs. Increasing collection time and spectral averaging increases the time it takes to gather data, thereby forcing longer wait times between information (e.g. concentration measurement) outputs.

To better compare the effects of changing collection time and spectral averaging, the laser power for the red, green, and blue systems were set to different levels to maximize the signal of each laser (220 mW, 20 mW, and 35 mW respectively). The nitrate and oxalate sample subset was then measured on all three systems under variable collection times and number of spectra averaged. Resulting LODs can be seen in Table 3-1 along with performance evaluation in section 3.3. As examples of the impacts of altering collection time and spectral averaging, Figure 3-3 and Figure 3-4 present measured spectra under the varied conditions for all three Raman systems.

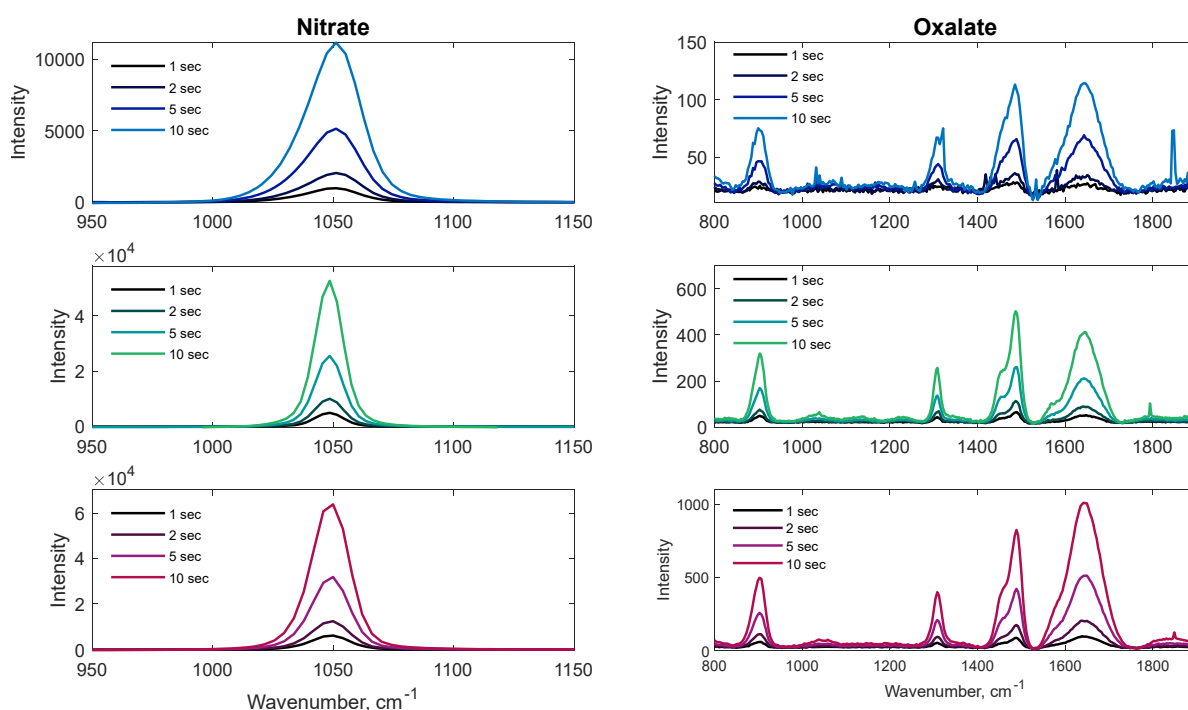


Figure 3-3. Raman spectra of 3 M nitrate (left) and 0.15 M oxalate (right) measured on the 405 nm (top), 532 nm (middle), and 671 nm (bottom) systems as collection time is varied from 1-10 seconds. On all three Raman systems spectral intensity increases with collection time. Note, lasers were set to dissimilar power settings

Note, Figures 3-3 and 3-4 present fingerprints from common waste species (nitrate and oxalate) that display strong and weak Raman fingerprints, respectively. Similar improvement of signal intensity as Raman laser wavelength is decreased can be seen for either chemical target. However, the impact is more notable in the weaker species, oxalate, because the ratio of signal to noise is very clearly improved.

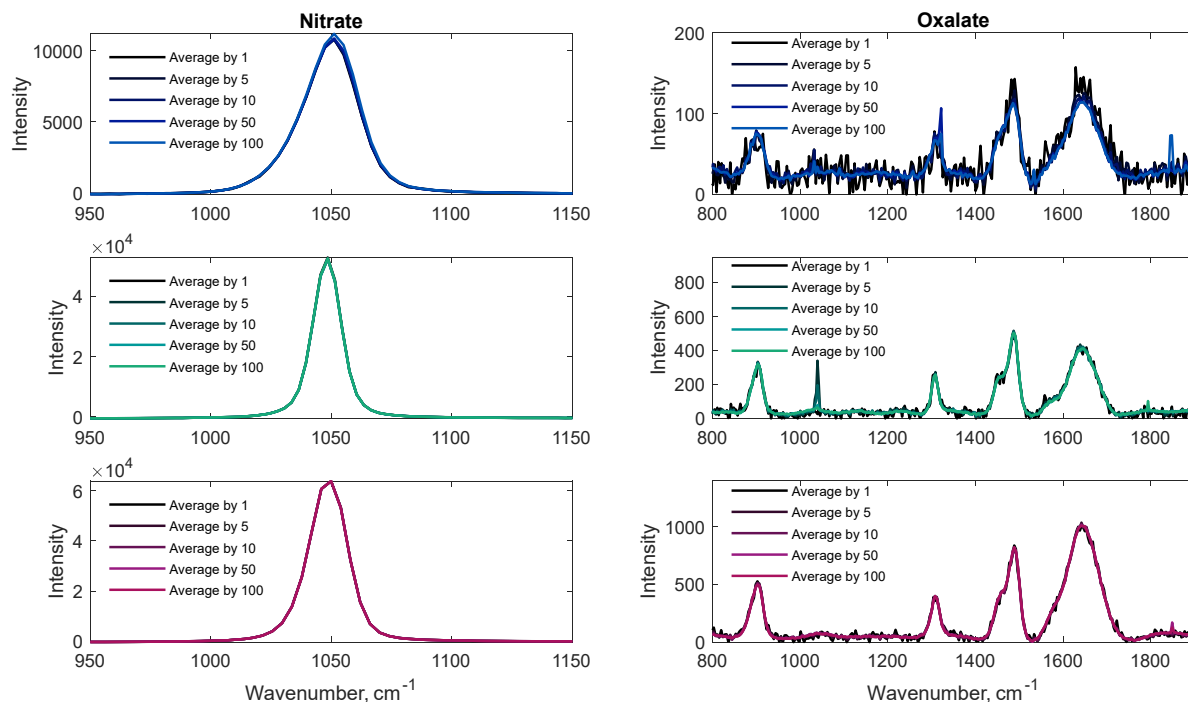


Figure 3-4. Raman spectra of 3 M nitrate (left) and 0.15 M oxalate (right) measured on the 405 nm (top), 532 nm (middle), and 671 nm (bottom) systems as averaging rate is varied from 1 to 100. On all three Raman systems the signal to noise ratio improves as averaging rate increases

3.3 Final notes on optimized parameters and anticipated limits of detection

Limits of detection were calculated using equation 3-1:

$$\text{LOD} = \frac{3s}{m} \quad \text{Eq. 3-1}$$

Where s is the noise of the blank and m is the slope of the line obtained by plotting the peak intensity versus concentration (Harris 2007).

Table 3-1 below presents the calculated LODs for the chemical species of the nitrate and oxalate subset as a function of laser system and collection parameters, as described in sections above. Overall, general trends indicate LODs improve as excitation laser wavelength is reduced in wavelength, from 671 to 532, and then 405 nm, under conditions of similar laser power for each. Additionally, results improve as collection and averaging time increase, especially for the lower signal oxalate spectra where the signal-to-noise is lower. There was up to a 12x observed improvement in oxalate LOD increasing the integration time from 1 sec to 10 sec and up to a 72x improvement by increasing the averaging from 1 to 10. Further increasing averaging from 1 to 100 improved the oxalate LOD by as much as 2000x.

Table 3-1. LOD values for nitrate and oxalate varying laser power, integration time, and spectral averaging for the 405, 532, and 671 nm excitation lasers. Spectral preprocessing included a 1st derivative, normalizing to the water band, followed by mean centering.

Analyte	Excitation Wavelength, nm	Laser Power, mW	Integration Time, sec	Average 1	Average 5	Average 10	Average 50	Average 100
NO ₃ ⁻	405	80	0.5	65.4·10 ⁻⁴	22.2·10 ⁻⁴	13.9·10 ⁻⁴	2.88·10 ⁻⁴	1.92·10 ⁻⁴
	405	35	1	703·10 ⁻⁴	325·10 ⁻⁴	187·10 ⁻⁴	27.4·10 ⁻⁴	6.38·10 ⁻⁴
	405	35	2	426·10 ⁻⁴	157·10 ⁻⁴	100·10 ⁻⁴	10.1·10 ⁻⁴	3.08·10 ⁻⁴
	405	35	5	129·10 ⁻⁴	44.6·10 ⁻⁴	34.7·10 ⁻⁴	5.79·10 ⁻⁴	0.90·10 ⁻⁴
	405	35	10	87.9·10 ⁻⁴	33.0·10 ⁻⁴	17.4·10 ⁻⁴	2.11·10 ⁻⁴	1.53·10 ⁻⁴
	532	100	0.5	63.7·10 ⁻⁴	40.3·10 ⁻⁴	19.3·10 ⁻⁴	6.05·10 ⁻⁴	2.13·10 ⁻⁴
	532	20	1	162·10 ⁻⁴	82.1·10 ⁻⁴	42.6·10 ⁻⁴	6.62·10 ⁻⁴	1.31·10 ⁻⁴
	532	20	2	90.9·10 ⁻⁴	32.6·10 ⁻⁴	27.2·10 ⁻⁴	1.94·10 ⁻⁴	1.22·10 ⁻⁴
	532	20	5	50.7·10 ⁻⁴	12.7·10 ⁻⁴	10.5·10 ⁻⁴	1.04·10 ⁻⁴	0.64·10 ⁻⁴
	532	20	10	19.1·10 ⁻⁴	9.50·10 ⁻⁴	7.22·10 ⁻⁴	0.62·10 ⁻⁴	0.28·10 ⁻⁴
	671	120	0.5	378·10 ⁻⁴	194·10 ⁻⁴	142·10 ⁻⁴	42.0·10 ⁻⁴	21.5·10 ⁻⁴
	671	220	1	124·10 ⁻⁴	67.2·10 ⁻⁴	36.6·10 ⁻⁴	3.81·10 ⁻⁴	1.67·10 ⁻⁴
	671	220	2	91.5·10 ⁻⁴	25.4·10 ⁻⁴	20.4·10 ⁻⁴	1.85·10 ⁻⁴	0.19·10 ⁻⁴
	671	220	5	20.8·10 ⁻⁴	21.9·10 ⁻⁴	7.32·10 ⁻⁴	1.63·10 ⁻⁴	0.25·10 ⁻⁴
	671	220	10	21.1·10 ⁻⁴	5.68·10 ⁻⁴	4.35·10 ⁻⁴	0.91·10 ⁻⁴	0.31·10 ⁻⁴
C ₂ O ₄ ²⁻	405	80	0.5	392·10 ⁻⁴	128·10 ⁻⁴	132·10 ⁻⁴	59.3·10 ⁻⁴	8.79·10 ⁻⁴
	405	35	1	1960·10 ⁻⁴	3020·10 ⁻⁴	2670·10 ⁻⁴	290·10 ⁻⁴	124·10 ⁻⁴
	405	35	2	2170·10 ⁻⁴	1940·10 ⁻⁴	1210·10 ⁻⁴	130·10 ⁻⁴	25.8·10 ⁻⁴
	405	35	5	4570·10 ⁻⁴	554·10 ⁻⁴	242·10 ⁻⁴	54.4·10 ⁻⁴	22.5·10 ⁻⁴
	405	35	10	863·10 ⁻⁴	312·10 ⁻⁴	190·10 ⁻⁴	23.0·10 ⁻⁴	25.2·10 ⁻⁴
	532	100	0.5	610·10 ⁻⁴	441·10 ⁻⁴	213·10 ⁻⁴	37.5·10 ⁻⁴	16.8·10 ⁻⁴
	532	20	1	1780·10 ⁻⁴	511·10 ⁻⁴	368·10 ⁻⁴	63.5·10 ⁻⁴	9.68·10 ⁻⁴
	532	20	2	756·10 ⁻⁴	237·10 ⁻⁴	130·10 ⁻⁴	19.5·10 ⁻⁴	5.95·10 ⁻⁴
	532	20	5	187·10 ⁻⁴	97.7·10 ⁻⁴	49.2·10 ⁻⁴	6.61·10 ⁻⁴	3.32·10 ⁻⁴
	532	20	10	3670·10 ⁻⁴	96.6·10 ⁻⁴	50.6·10 ⁻⁴	7.90·10 ⁻⁴	1.82·10 ⁻⁴
	671	120	0.5	1600·10 ⁻⁴	674·10 ⁻⁴	618·10 ⁻⁴	222·10 ⁻⁴	37.0·10 ⁻⁴
	671	220	1	624·10 ⁻⁴	163·10 ⁻⁴	247·10 ⁻⁴	64.9·10 ⁻⁴	12.5·10 ⁻⁴
	671	220	2	523·10 ⁻⁴	197·10 ⁻⁴	114·10 ⁻⁴	14.1·10 ⁻⁴	4.96·10 ⁻⁴
	671	220	5	422·10 ⁻⁴	113·10 ⁻⁴	88.6·10 ⁻⁴	18.2·10 ⁻⁴	2.66·10 ⁻⁴
	671	220	10	135·10 ⁻⁴	57.7·10 ⁻⁴	36.6·10 ⁻⁴	6.43·10 ⁻⁴	1.56·10 ⁻⁴

Initial analysis would suggest that collection parameters used for optical training set development should focus on the blue system with the longest collection time and highest spectral averaging.

However, there are key factors not emphasized by the nitrate and oxalate subset that need to be highlighted before settling on collection parameters.

These can be highlighted with some initial spectra collected of real Hanford tank process samples, which can be seen in Section 5.0. As an overview, the fluorescence background observed in some oxalate samples can become a serious challenge for the blue system in some real waste samples. With this in mind, it appears focusing on the green system may be the most beneficial. Ultimately, complete training sets were collected on all three Raman systems. Benefits of this are discussed in the modeling Section 4.0. Collection parameters were chosen based off results presented in Table 3-1. All three systems were set to approximately 100 mW, spectral averaging was set to 100, though collection time was reduced to 0.5 s to avoid saturation of detectors.

4.0 Collection of training sets and building of chemometric models

Following optimization of collection parameters, full training sets were collected on the red, green, and blue Raman systems. Training sets were designed to focus heavily on low concentration ranges, but included high data points to support efficient model training. Table 4-1 below lists the target analytes and concentration ranges included in the training set. Note, the full training set included 10 target analytes, all of which are common in tank waste and several of which pose processing concerns in both low and high concentration stages of tank processing.

Table 4-1. Training set target analytes and concentration ranges

Analyte	Concentration, M
NaOH	0.05 - 8
Al(OH) ₄ ⁻	0.001 - 1 M
CO ₃ ²⁻	0.01 - 2 M
CrO ₄ ²⁻	0.0005 - 1 M
NO ₃ ⁻	0.01 - 3 M
NO ₂ ⁻	0.01 - 1 M
PO ₄ ³⁻	0.0005 - 0.5 M
SO ₄ ²⁻	0.0005 - 0.75 M
C ₂ O ₄ ²⁻	0.0005 - 0.15 M
NH ₄ ⁺	0.005 - 5 M

The full training set included species that were not in the nitrate and oxalate subset. Figures below present examples of optical fingerprints of targets, along with single variate calibration curves used to calculate LODs of the targets. Table 4-2 then presents the LODs of all targets on the red, green, and blue Raman systems under the collection parameters used for the training set. Note, the single variate quantification approach is simplistic, and while it can provide some powerful insight into system behavior, it is not robust enough to be applied in complex solutions. Following sections will provide further insight into observed spectral complexity and advanced analysis approaches that can accurately handle this data while minimizing uncertainty in quantification.

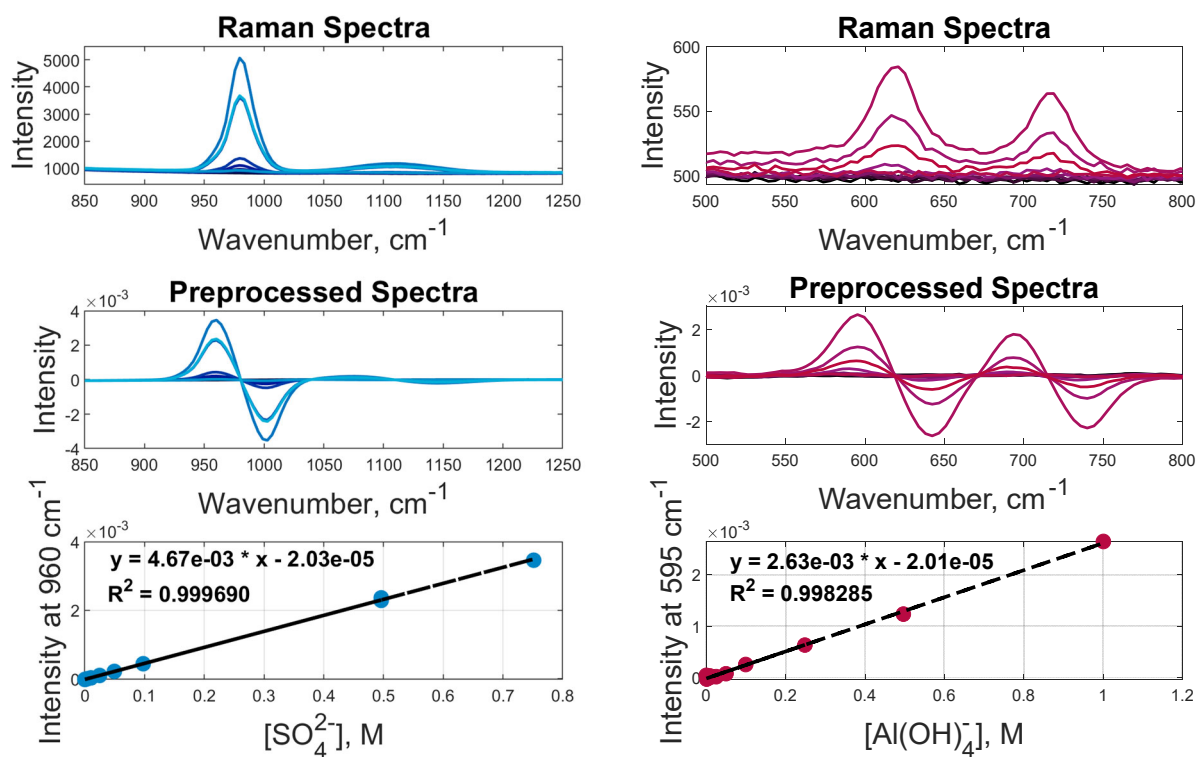


Figure 4-1. Examples of spectral signatures (top) and preprocessed spectra (middle) used for single variate calibration curves (bottom) for the sulfate band for the 405 nm system (left) and aluminate band on the 671 nm system (right).

Table 4-2. LODs for target analytes on the red, green, and blue systems. Spectral preprocessing included a 1st derivative, normalizing to the water band, followed by mean centering.

Analyte	Excitation Wavelength, nm	Laser Power, mW	Integration Time, sec	Average 1	Average 5	Average 10	Average 50	Average 100
NaOH	405	80	0.5	1020·10 ⁻⁴	280·10 ⁻⁴	230·10 ⁻⁴	136·10 ⁻⁴	26.0·10 ⁻⁴
	532	100	0.5	2480·10 ⁻⁴	708·10 ⁻⁴	535·10 ⁻⁴	117·10 ⁻⁴	47.2·10 ⁻⁴
	671	120	0.5	5370·10 ⁻⁴	3080·10 ⁻⁴	2480·10 ⁻⁴	1080·10 ⁻⁴	458·10 ⁻⁴
Al(OH) ₄ ⁻	405	80	0.5	247·10 ⁻⁴	149·10 ⁻⁴	100·10 ⁻⁴	21.0·10 ⁻⁴	11.9·10 ⁻⁴
	532	100	0.5	445·10 ⁻⁴	199·10 ⁻⁴	192·10 ⁻⁴	106·10 ⁻⁴	26.3·10 ⁻⁴
	671	120	0.5	2150·10 ⁻⁴	1330·10 ⁻⁴	878·10 ⁻⁴	206·10 ⁻⁴	90.4·10 ⁻⁴
CO ₃ ²⁻	405	80	0.5	125·10 ⁻⁴	56.7·10 ⁻⁴	51.3·10 ⁻⁴	15.0·10 ⁻⁴	2.85·10 ⁻⁴
	532	100	0.5	204·10 ⁻⁴	60.7·10 ⁻⁴	50.8·10 ⁻⁴	15.7·10 ⁻⁴	6.65·10 ⁻⁴
	671	120	0.5	988·10 ⁻⁴	406·10 ⁻⁴	317·10 ⁻⁴	91.4·10 ⁻⁴	43.4·10 ⁻⁴
CrO ₄ ²⁻	405	80	0.5	21.9·10 ⁻⁴	6.91·10 ⁻⁴	2.02·10 ⁻⁴	0.31·10 ⁻⁴	0.058·10 ⁻⁴
	532	100	0.5	11.0·10 ⁻⁴	6.92·10 ⁻⁴	5.09·10 ⁻⁴	0.011·10 ⁻⁴	0.52·10 ⁻⁴
	671	120	0.5	115·10 ⁻⁴	70.9·10 ⁻⁴	52.8·10 ⁻⁴	11.1·10 ⁻⁴	4.10·10 ⁻⁴
NO ₃ ⁻	405	80	0.5	65.4·10 ⁻⁴	22.3·10 ⁻⁴	13.9·10 ⁻⁴	2.88·10 ⁻⁴	1.92·10 ⁻⁴
	532	100	0.5	63.8·10 ⁻⁴	40.3·10 ⁻⁴	19.3·10 ⁻⁴	6.05·10 ⁻⁴	2.13·10 ⁻⁴
	671	120	0.5	378·10 ⁻⁴	193·10 ⁻⁴	142·10 ⁻⁴	42.1·10 ⁻⁴	21.5·10 ⁻⁴
NO ₂ ⁻	405	80	0.5	211·10 ⁻⁴	88.4·10 ⁻⁴	49.8·10 ⁻⁴	23.9·10 ⁻⁴	3.55·10 ⁻⁴
	532	100	0.5	700·10 ⁻⁴	221·10 ⁻⁴	162·10 ⁻⁴	58.6·10 ⁻⁴	17.8·10 ⁻⁴
	671	120	0.5	1640·10 ⁻⁴	711·10 ⁻⁴	544·10 ⁻⁴	333·10 ⁻⁴	123·10 ⁻⁴
PO ₄ ³⁻	405	80	0.5	340·10 ⁻⁴	81.3·10 ⁻⁴	61.9·10 ⁻⁴	41.0·10 ⁻⁴	6.58·10 ⁻⁴
	532	100	0.5	297·10 ⁻⁴	135·10 ⁻⁴	117·10 ⁻⁴	40.3·10 ⁻⁴	8.67·10 ⁻⁴
	671	120	0.5	1970·10 ⁻⁴	474·10 ⁻⁴	446·10 ⁻⁴	264·10 ⁻⁴	33.3·10 ⁻⁴
SO ₄ ²⁻	405	80	0.5	94.7·10 ⁻⁴	32.3·10 ⁻⁴	16.7·10 ⁻⁴	6.51·10 ⁻⁴	2.89·10 ⁻⁴
	532	100	0.5	83.0·10 ⁻⁴	61.2·10 ⁻⁴	35.9·10 ⁻⁴	6.11·10 ⁻⁴	2.74·10 ⁻⁴
	671	120	0.5	443·10 ⁻⁴	198·10 ⁻⁴	131·10 ⁻⁴	48.6·10 ⁻⁴	22.3·10 ⁻⁴
C ₂ O ₄ ²⁻	405	80	0.5	392·10 ⁻⁴	128·10 ⁻⁴	132·10 ⁻⁴	59.3·10 ⁻⁴	8.79·10 ⁻⁴
	532	100	0.5	610·10 ⁻⁴	441·10 ⁻⁴	213·10 ⁻⁴	37.5·10 ⁻⁴	16.9·10 ⁻⁴
	671	120	0.5	1600·10 ⁻⁴	674·10 ⁻⁴	618·10 ⁻⁴	222·10 ⁻⁴	37.0·10 ⁻⁴
NH ₄ OH	405	80	0.5	811·10 ⁻⁴	606·10 ⁻⁴	326·10 ⁻⁴	86.9·10 ⁻⁴	22.0·10 ⁻⁴
	532	100	0.5	1590·10 ⁻⁴	804·10 ⁻⁴	447·10 ⁻⁴	98.6·10 ⁻⁴	51.0·10 ⁻⁴
	671	120	0.5	5240·10 ⁻⁴	1190·10 ⁻⁴	1030·10 ⁻⁴	275·10 ⁻⁴	175·10 ⁻⁴

Several chemometric modeling approaches were assessed for application to this system. Partial least-square (PLS) regression was utilized for the analysis of this work. This technique has been applied to other studies of complex systems (Lines et al. 2019, Lackey et al. 2020, Casella et al. 2016). Some of the analytes which produced a lower Raman signal and where the spectral signature overlapped with the signatures of several other species (oxalate, carbonate, nitrite,

hydroxide, phosphate) required the use of a locally weighted regression (LWR) model utilizing 30 of the most similar spectra to use in the PLS model instead of the entire training set. Spectra were preprocessed by applying a 1st derivative, normalizing to the water band, and then applying a mean centering before further analysis. Cross validation was done using venetian blinds with 10 data splits and 1 sample per blind. Several modeling methods were compared to determine the best approach for this system. In all models, each analyte was modeled separately using a limited spectral range which encompassed only the spectral signature range for each analyte. By doing this, the model is better able to ignore contributions from other analytes which have signatures in different wavenumber regions. In the first modeling method, each laser system was analyzed separately which can provide a comparison of the effectiveness of each laser system in measuring each analyte. Example modeling results are shown in Figure 4-2 for high signal (chromate and nitrate) and low signal (oxalate and aluminate) species. Model statistics included the root-mean-error of calibration (RMSEC) which is a measure of the model's ability to predict the known concentrations of the training set, and the root-mean-error of cross-validation (RMSECV) is a measure of model's ability to predict concentrations of training set data left out of the model during cross-validation. The statistics for this model are shown in Table 4-3.

The second modeling method involved combining all laser data together into a multiblock model. The results for these multiblock models for all analytes are show in

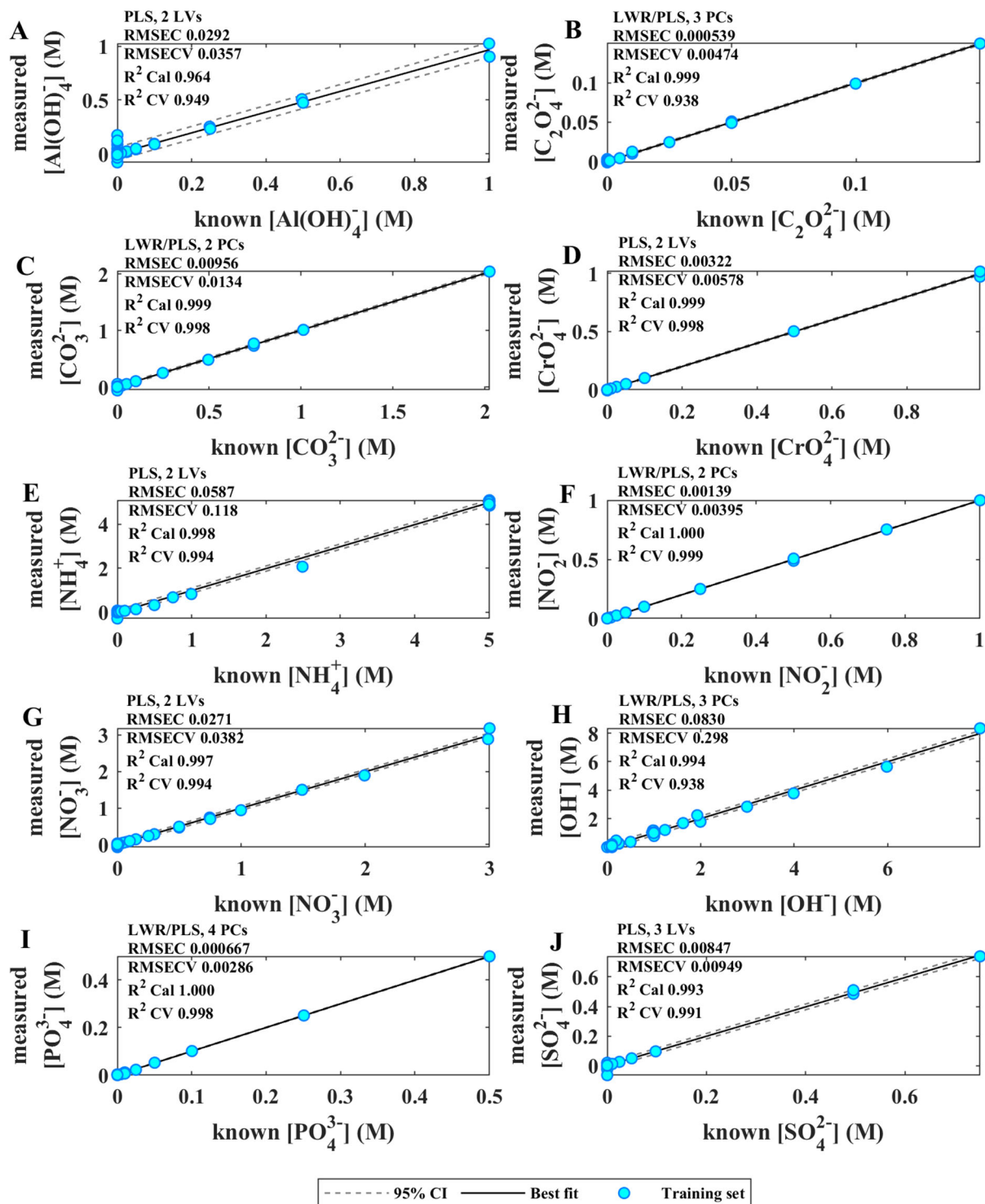


Figure 4-3 and the modeling statistics are presented in Table 4-4. In this modeling method, the model can use all available information from the three laser systems to build the models. This can help the model compensate for weaknesses of specific laser systems by emphasizing other laser system data. For example, the 405 nm excitation wavelength is absorbed by yellow chromate solutions resulting in a loss of signal produced by that laser system. This can be seen in Figure 4-2A where the parity plot for the 405 nm system is not linear. By combining the data

from all three laser systems, the model can emphasize the data from the 532 and 671 nm systems and results in a linear parity plot shown in

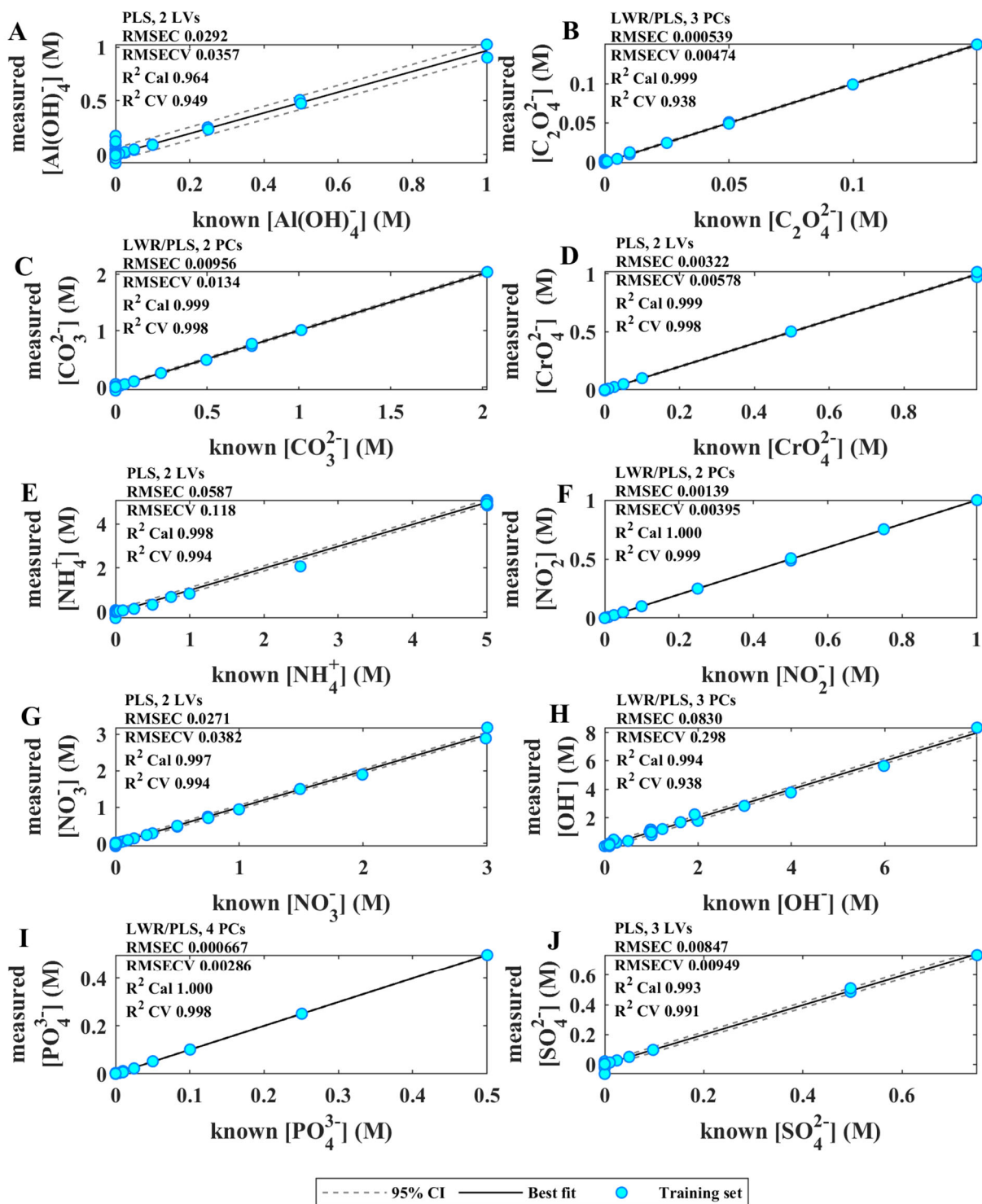


Figure 4-3D.

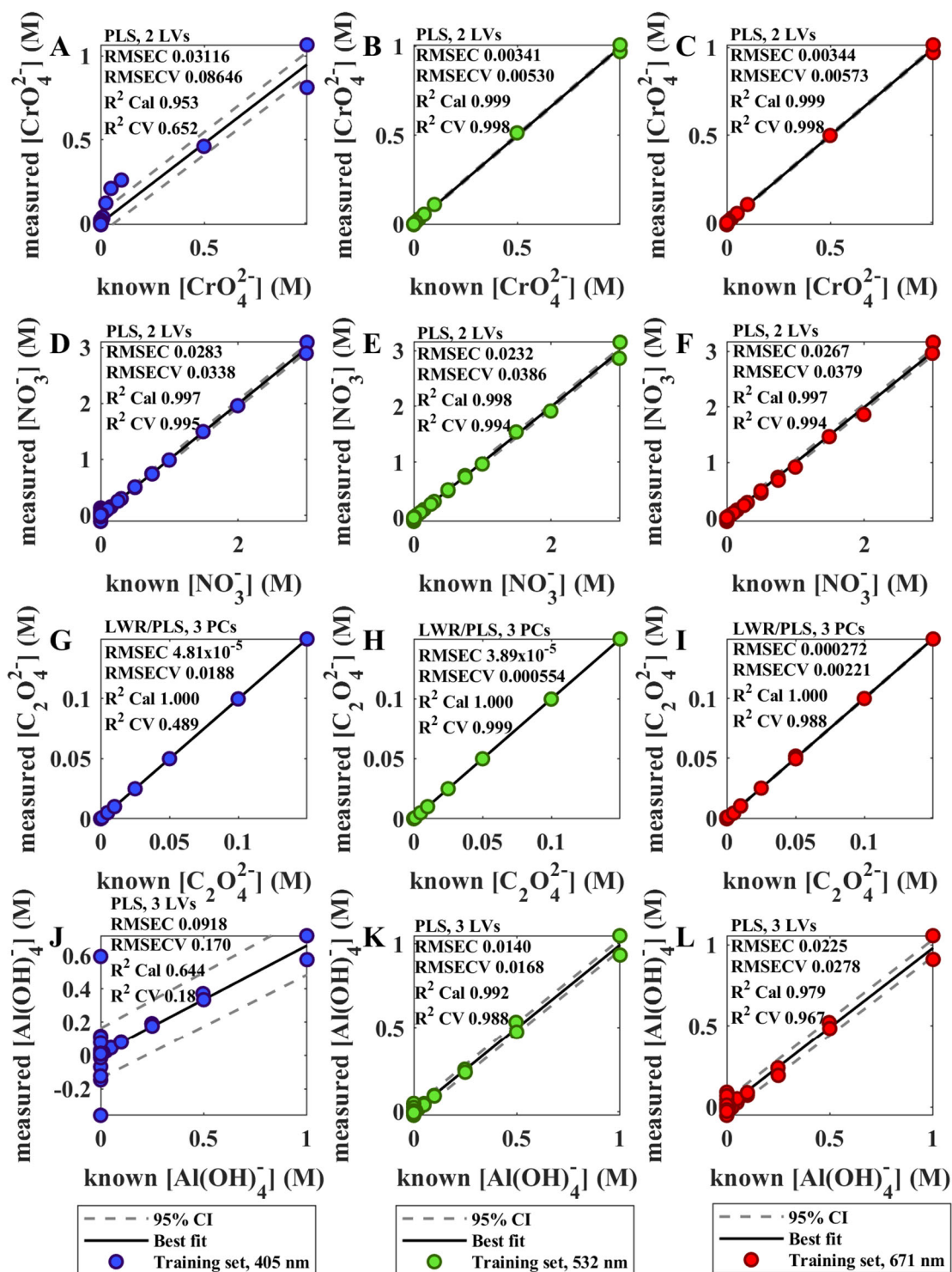


Figure 4-2. Parity plots of training set models built for each laser system separately and analyzing analytes separately. These example results include CrO_4^{2-} (A-C), NO_3^- (D-F), $\text{C}_2\text{O}_4^{2-}$ (G-I), and Al(OH)_4^- (J-L).

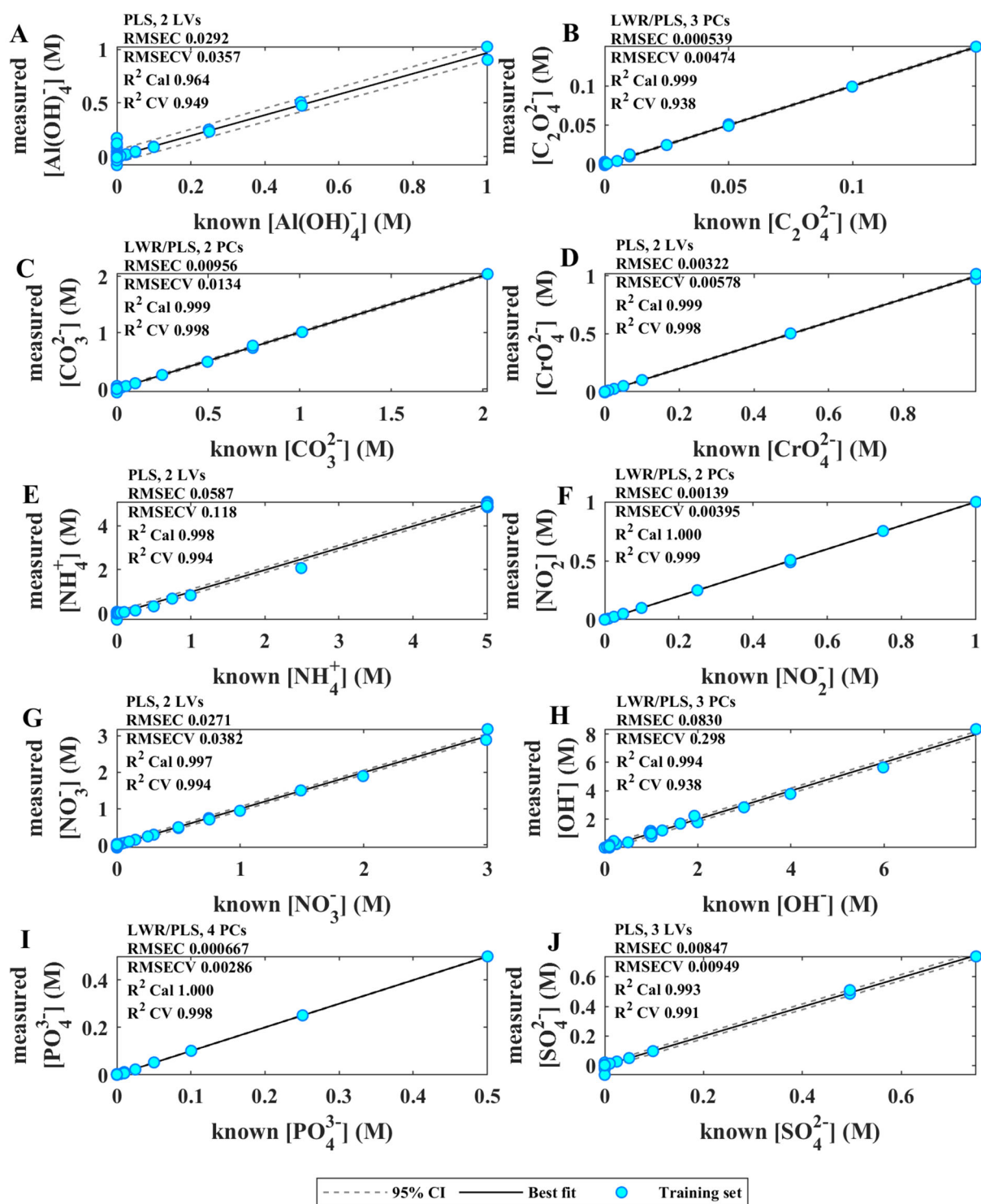


Figure 4-3. Parity plots of training set models built using multiblock modeling of all 3 laser systems and modeling all analytes separately.

Table 4-3. Modeling statistics for the models shown in Figure 4-2: RMSECV=uncertainty, M

Analyte	LVs/ PCs	RMSEC / RMSECV (M)			R ² (cal) / R ² (CV)		
		405 nm	532 nm	671 nm	405 nm	532 nm	671 nm
CrO ₄ ²⁻	2	0.0311646/ 0.0864587	0.00340662 / 0.00530473	0.00343803/ 0.00573472	0.952595 / 0.652312	0.999423/ 0.998398	0.999423/ 0.998398
NO ₃ ⁻	2	0.0283222/ 0.0338791	0.0232122/ 0.0385515	0.0266677/ 0.0379185	0.996612/ 0.995158	0.997724/ 0.993931	0.996997/ 0.994171
C ₂ O ₄ ²⁻	3	0.000048145/ 0.0188283	0.000038941/ 0.000554652	0.000272238/ 0.00220596	0.999993/ 0.488593	0.999996/ 0.999173	0.999791/ 0.988088
Al(OH) ₄ ⁻	3	0.0917895/ 0.170208	0.0139981/ 0.0168246	0.022476/ 0.0278428	0.644031/ 0.181233	0.991721/ 0.988056	0.978657/ 0.967416

Table 4-4. Modeling statistics for the models shown in Figure 4-3: RMSECV=uncertainty, M

Analyte	LVs/PCs	RMSEC / RMSECV (M)	R ² (cal)/R ² (CV)
OH ⁻	2	0.0829918/0.297851	0.99431/0.93796
Al(OH) ₄ ⁻	2	0.0291948/0.035735	0.96399/0.94885
CO ₃ ²⁻	2	0.0095627/0.013426	0.99850/0.99776
CrO ₄ ²⁻	2	0.0032201/0.005783	0.99949/0.99837
NO ₃ ⁻	2	0.0271728/0.038207	0.99688/0.99398
NO ₂ ⁻	2	0.0013885/0.003948	0.99990/0.99920
PO ₄ ³⁻	4	0.0006670/0.002860	0.99985/0.99785
SO ₄ ²⁻	3	0.0084707/0.009485	0.99265/0.99078
C ₂ O ₄ ²⁻	3	0.0005393/0.004740	0.99917/0.93767
NH ₄ ⁺	2	0.0587489/0.117749	0.99845/0.99370

In chemometric modeling, the RMSECV is defined as the root-mean-square-error between the measured and known values used in cross validation, and can be interpreted as the uncertainty (or the ± concentration value with the same measurement units as the training set, M here) for quantification results. (Faber and Bro 2002) As seen in Tables 4-3 and 4-4, RMSECV values indicate lower uncertainty for several of the target species compared to others. This is clearer in subsequent sections where these uncertainty values can be compared to anticipated concentrations within real and simulated Hanford samples. Furthermore, an improvement in uncertainty is generally observed in the single Raman laser models following the pattern of red>green>blue. Interestingly, multiblock models generally perform at least as well as the green single system models, and in some cases perform better than all single Raman system models.

5.0 Application to Hanford tank processing samples and simulants

The PNNL team had unique opportunities to capture optical data on several real-tank processing samples¹. Figure 5-1 presents the spectra of the characterized samples before application of any preprocessing. Application of models to real sample data is an ideal way to determine model performance. However, because the number and variability of real samples was limited, additional simulant samples of Hanford tanks as well as additional validation samples were created and integrated into the model validation data set. The additional validation samples were designed to encompass the low concentration ranges of each analyte to better determine the lower limit of the models. Table 5-1 describes all the samples in the validation set, including the real processing samples, simulants, and additional validation samples. Note that for the real processing samples, some analyte concentrations were determined by elemental analysis (Al, Cr, P, S) and assumed to be present in solution as the molecular form presented in Table 5-1 (Al(OH)₄⁻, CrO₄²⁻, PO₄³⁻, SO₄²⁻).

Table 5-1. Samples included in the validation set with molar concentrations of each analyte.

Sample	OH ⁻	Al(OH) ₄ ⁻	CO ₃ ²⁻	CrO ₄ ²⁻	NO ₃ ⁻	NO ₂ ⁻	PO ₄ ³⁻	SO ₄ ²⁻	C ₂ O ₄ ²⁻
AP-105 off-gas condensate	---	0.00135	---	2.21E-04	0.276	---	8.07E-05	8.92E-04	---
AP-105 off-gas evaporate	---	0.0135	---	0.00221	2.76	---	0.000807	0.00892	---
AP-105	1.24	0.523	---	0.00656	1.89	1.38	0.00882	0.0228	0.00180
AP-107 evaporator condensate	---	1.86E-04	---	4.81E-06	8.10E-05	1.09E-04	5.29E-05	5.23E-05	---
AP-107 and evaporator concentrate	---	0.260	---	0.00671	0.336	0.276	0.0201	0.0432	---
AW-102	---	0.432	---	0.00987	1.74	1.16	0.0233	0.0250	0.00253
Simulant AP-105	1.41	0.640	0.440	0.00701	1.72	1.28	0.0201	0.0360	0.00201
Simulant S-109EF	2.04	0.520	0.611	0.0789	4.28	0.825	0.0249	0.140	0
Simulant S-109LF	0.451	0.0439	0.240	0.0182	1.54	0.077	0.0550	0.158	0
Simulant AY-102	1.56	1.02	1.03	0	0.057	0.001072	0.0110	0.0180	0.0329
Simulant AP-101	3.28	0.452	0.470	0	2.01	0.947	0.00833	0.0293	0.00982
Validation 1	1.49	0	0	0.00100	0.0150	0	0.0747	0	0.0150
Validation 2	0.752	0.00200	0.0200	0	0	0.0150	0	0	9.97E-04
Validation 3	0.498	0.149	0	0	0.747	0.198	0	0.0499	0
Validation 4	1.48	0.200	0.0501	0.0300	0	0.100	0	0	0
Validation 5	0.500	0	0.151	0	0.400	0	0.0998	0.00102	0
Validation 6	0.317	0.150	0	0	0.150	0	0	0.0801	0.00750
Validation 7	0.747	0.0750	0	0	0.225	0.0300	0.0400	0	0.0200
Validation 8	0.105	0.00200	0.396	0	0.155	0	0.00100	0.0990	0
Validation 9	0.991	0.248	0.396	0	0.462	0.199	0.0991	0.00102	0.0198
Validation 10	1.00	0.00401	0.150	0.00100	0.404	0.0998	0.00100	0.0990	0.00747

¹ These samples were collected during testing on the PNNL Radioactive Waste Test platform.
 --- Analyte concentrations not measured during analysis.

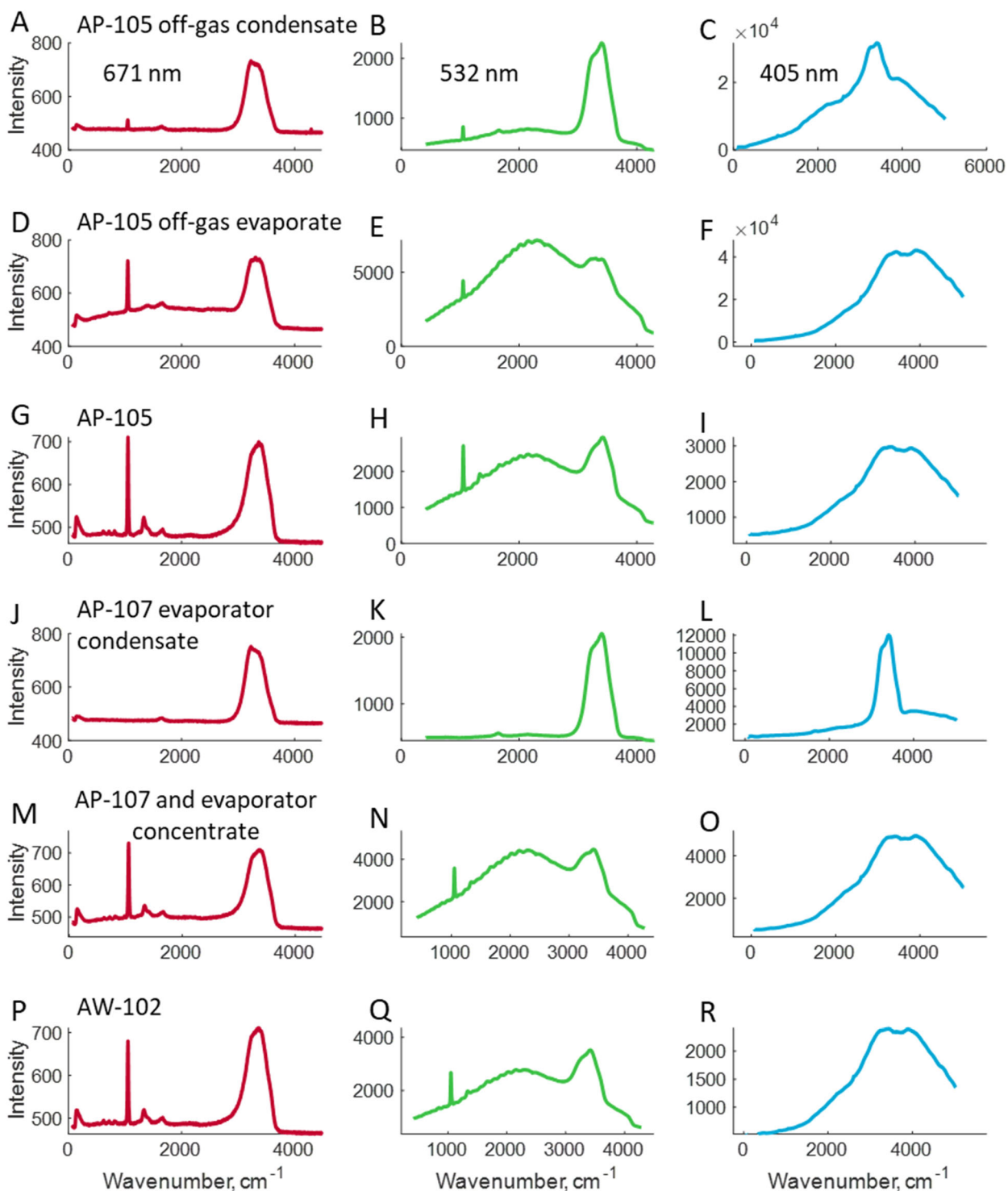


Figure 5-1. Raman spectra of real-tank processing samples measured with the 671 nm (left), 532 nm (middle) and 405 nm (right) systems. Each spectrum was measured at 0.1 sec integration time and represents an average of 200 spectra.

Spectra of the real Hanford processing samples help highlight one of the challenges faced in utilizing lower excitation wavelength Raman systems. Firstly, fluorescence is observed in several samples with the greatest interference occurring in the 405 nm, or blue Raman system, data, as seen in the last (blue) column of Figure 5-1. The 532 nm, or green Raman system, shows some fluorescence interference but at a significantly lower level than the blue system. Secondly, at least one common tank species, chromate being the key example in this data set, strongly absorbs the 405 nm excitation light, making it difficult to quantify chromate or solutions containing high concentrations of chromate with the blue system. The first challenge of fluorescence can be mitigated by preprocessing data. Figure 5-2 contains examples of this where the interferences observed in Figure 5-1 are significantly reduced on the preprocessed data of Figure 5-2.

Ultimately the most important question is how well the chemometric models described in the previous section can measure target analytes in the validation set. Figure 5-3 presents parity plots demonstrating application of models to validation set data. Several models perform well, including aluminate, chromate, nitrate, nitrite, phosphate, and sulphate models. Some outliers are observed even in these model results. In these cases, spectral results clearly indicate the presence of the chemical targets. This project team is working with the test platform team to ensure sample characterization values presented here represent the same process analyzed samples. Results for oxalate and carbonate show stronger deviations from known values. In the case of oxalate, spectral signatures do not show any significant fingerprints for oxalate, despite anticipated concentration ranges well within measurable range. Here it is possible that some precipitation might have impacted solution composition by the time the on-line monitoring team was able to characterize the samples. Similarly, differences in pH between the training set and validation samples may have impacted carbonate results.

Quantitative model outputs combined with the uncertainty (RMSECV) values reported in Table 4-4 generally show excellent model performance for several key analytes within Hanford processing streams and demonstrate successful application to low concentration samples.

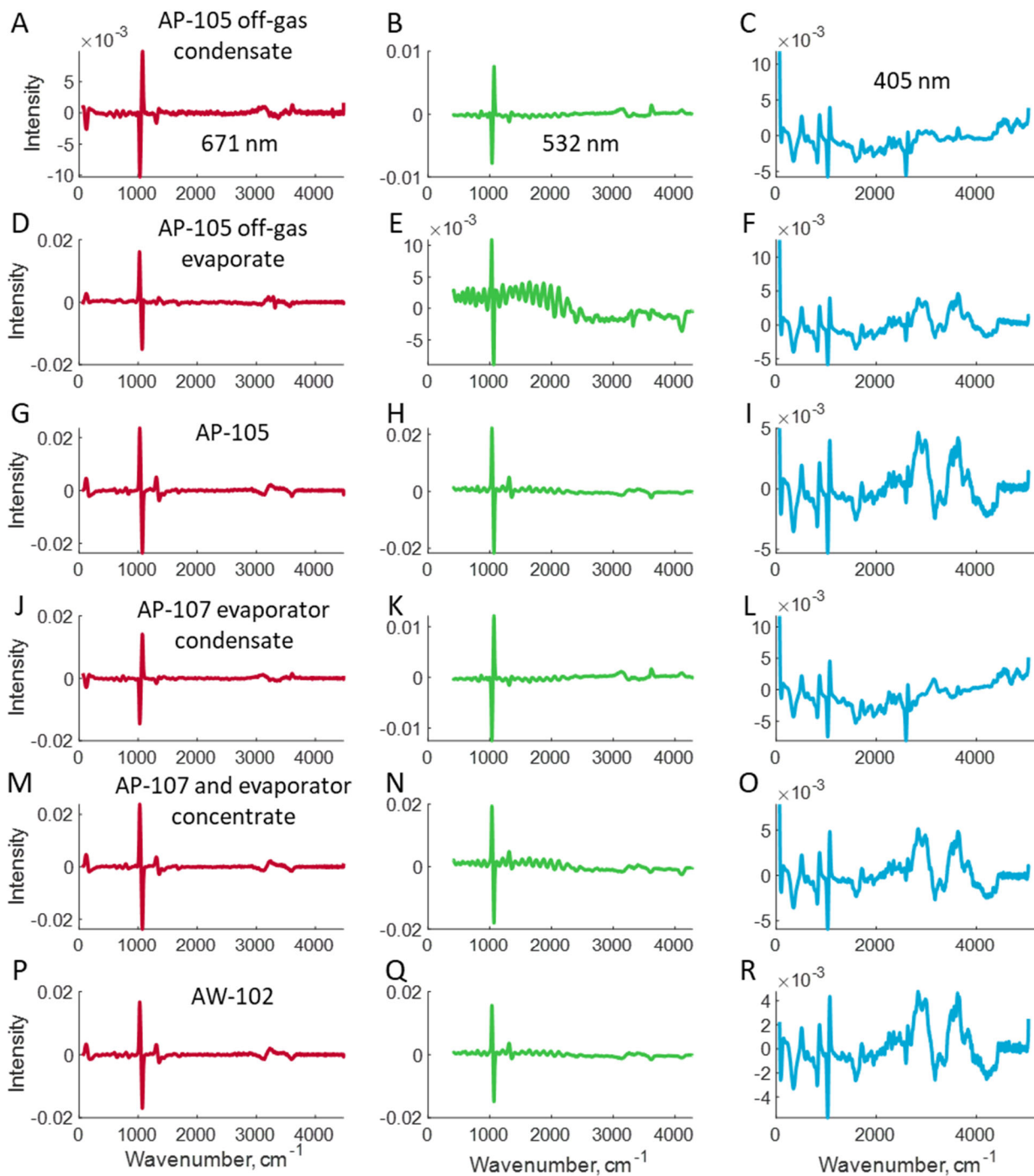


Figure 5-2. Preprocessed Raman spectra of real-tank processing samples measured with the 671 nm (left), 532 nm (middle) and 405 nm (right) systems. Preprocessing included: 1st derivative, normalization to the water band, and mean centering. Each spectrum was measured at 0.1 sec integration time and represents an average of 200 spectra.

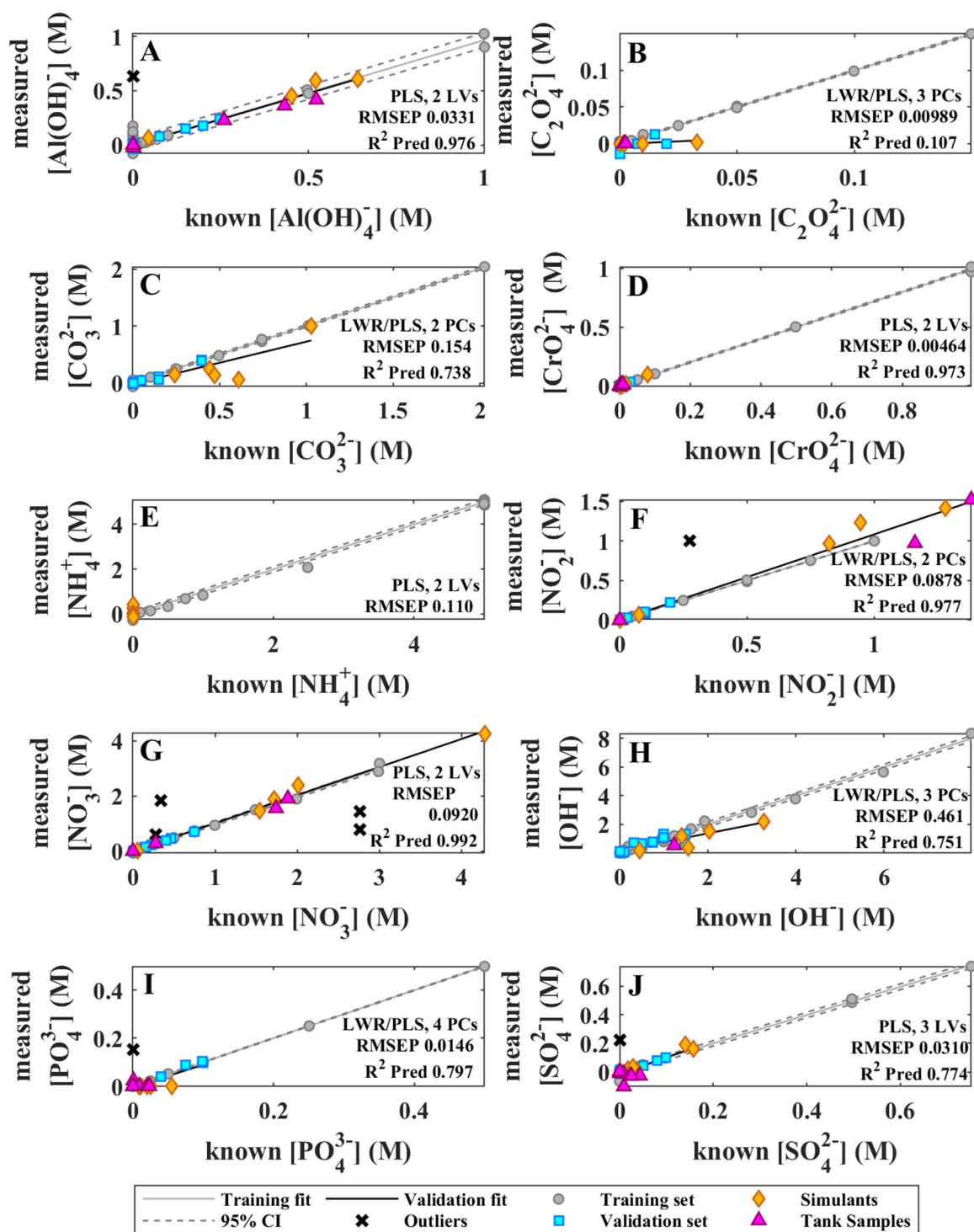


Figure 5-3. Parity plots of training set models overlaid with validation set results built using multiblock modeling of all 3 laser systems together.

Table 5-2. Comparison of known Hanford waste, waste concentrate, and evaporate samples used as analyte validation set concentrations compared to chemometrically measured concentrations.

Sample	Al(OH) ₄ ⁻	CrO ₄ ²⁻	NO ₃ ⁻	NO ₂ ⁻	PO ₄ ³⁻	SO ₄ ²⁻	C ₂ O ₄ ²⁻
AP-105 off-gas condensate known	0.00135	0.000221	0.276	---	8.07E-05	0.000892	---
Measured ±	-0.024 ±	0.0006 ±	0.288 ±	0.0000 ±	1.8E-05 ±	-0.0091 ±	-0.0035 ±
RMSECV	0.036	0.0058	0.038	0.0039	286E-05	0.0095	0.0047
AP-105 off-gas evaporate known	0.0135	0.00221	2.76	---	0.000807	0.00892	---
Measured ±	-0.089 ±	0.0092 ±	1.438 ±	0.0000 ±	0.0240 ±	-0.1019 ±	-0.1397 ±
RMSECV	0.036	0.0058	0.038	0.0039	0.0029	0.0095	0.0047
AP-105 known	0.523	0.00656	1.89	1.38	0.00882	0.0228	0.00180
Measured ±	0.417 ±	0.0037 ±	1.906 ±	1.5223 ±	0.0001 ±	-0.0284 ±	0.0000 ±
RMSECV	0.036	0.0058	0.038	0.0039	0.0029	0.0095	0.0047
AP-107 evaporator condensate known	0.000186	4.81E-06	8.10E-05	0.000109	5.29E-05	5.23E-05	---
Measured ±	-0.001 ±	1040E-06 ±	714E-05 ±	0.0000 ±	44.6E-05 ±	253E-05 ±	0.0056 ±
RMSECV	0.036	5783E-06	3821E-05	0.0039	286E-05	949E-05	0.0047
AP-107 and evaporator concentrate known	0.260	0.00671	0.336	0.276	0.0201	0.0432	---
Measured ±	0.228 ±	0.0107 ±	1.831 ±	1.0032 ±	0.0000 ±	-0.0262 ±	-0.0990 ±
RMSECV	0.036	0.0058	0.038	0.0039	0.0029	0.0095	0.0047
AW-102 known	0.432	0.00987	1.74	1.16	0.0233	0.0250	0.00253
Measured ±	0.362 ±	0.0099 ±	1.557 ±	0.9735 ±	0.0000 ±	-0.0277 ±	0.0000 ±
RMSECV	0.036	0.0058	0.038	0.0039	0.0029	0.0095	0.0047

6.0 Next steps for implementation into the Hanford Direct Feed Low Activity Waste processing

In FY21 PNNL combined optimized wavelength RAMAN systems with chemometric analysis, a form of supervised machine learning, to increase the sensitivity of the optical real-time systems. The use of chemometric analysis facilitates the transformation of data into information that can be used by a process operator to easily understand process conditions. The project team has experience not only in developing these systems, but also working with a small business partner to commercialize the equipment and chemometric models into systems that can be procured commercially and then maintained by the small business.

The next steps for using the Raman system in the DFLAW process are outlined below.

- Perform initial lab demonstration of in situ monitoring of solution with Raman spool piece in flow loop. This includes:
 - Establish necessary design features of Raman probe and spool piece:
 - Make design changes necessary to safely integrate Raman sensor and ensure compatibility with the intended online/in-tank deployment locations
 - Identify appropriate target analytes and determine if Raman sensitivity is appropriate for accurately quantifying targets in anticipated process concentration ranges
 - Design and build spool piece for insertion of Raman probe into flow loop, targeting design to integrate into jumper under future FY work
 - Enrich chemometric training set to expand applicably to additional tanks (building on previous AP-105 focus) and build chemometric models
 - Integrate spool piece and probe into flow loop, characterize probe response and test applicability of chemometric models
- Spool Design and Testing
 - Design and build spool piece for integrating Raman probe into flow loop test platform
 - Identify target analyte(s) and enrich training sets to include expanded data for enhanced applicability to tanks/processes. Build chemometric model(s) for real-time quantification of target analyte
 - This will include collection of spectral training set, building and validating model performance.
 - Collaborate with SMEs to verify spool piece design and integration plan are appropriate
- Finalize the Raman technology for DFLAW field use.

- Complete any on-line monitoring software modifications identified in FY22.
- Verify and validate automated analysis software.
- Complete safety evaluation(s) of Raman probe and deployment configuration (e.g., spool piece) that are necessary for field deployment.
- Integrate Raman spool piece and probe into flow loop test platform
- Complete demonstration tests of probe ability to detect analytes and real-time analysis software ability to quantify target analytes in real-time.
- Deploy for use.

7.0 Conclusions

On-line monitoring is a powerful tool to gain insight into chemical processes. Optical approaches such as Raman spectroscopy can provide chemical composition analysis, and uniquely identify and quantify several key constituents of Hanford waste, including nitrate, nitrite, carbonate, chromate, sulfate, phosphate, hydroxide, oxalate, ammonia, and aluminate. Furthermore, when optical approaches are paired with advanced analysis such as chemometric modeling, highly accurate data analysis can be achieved in real-time.

Automated data analysis such as this can be used to continuously monitor processes, enabling real-time control and verification of process conditions, reducing the need for costly grab sample collections. Work here demonstrated Raman spectroscopy coupled with chemometric analysis can be successfully applied to the analysis of 10 key analytes within Hanford waste streams. Specifically, optical instrument parameters such as Raman excitation wavelengths (671 nm, 532 nm, and 405 nm), spectral collection time, and averaging were optimized to obtain low limits of detection and enable application to low concentration waste streams. Several chemometric modeling approaches were explored, including models based solely on single excitation wavelengths as well as multiblock models built using data from all three Raman systems simultaneously.

Overall models accurately quantified multiple targets within both real and simulated tank processing samples. Most importantly, optimization of Raman data collection and chemometric modeling approaches enabled notable improvements in uncertainty of measured results. As an example, for nitrate, limits of detection were dropped substantially as laser wavelength was decreased from 671 nm to 405 nm. Further improvement was observed as collection parameters such as collection time and averaging were also increased. This sensitivity translated to reduced uncertainty (measured as the root mean square error of cross validation, RMSECV) when building chemometric models. Overall, results observed here show successful application of Raman-based monitoring approaches to the analysis of low concentration Hanford processing streams.

8.0 References

- Beebe, K.R., R.J. Pell, and M.B. Seasholtz. 1998. *Chemometrics: A Practical Guide*. New York: Wiley.
- Bro, R., and L. Elden. 2009. "PLS works." *Journal of Chemometrics* 23 (1-2):69-71.
- Bryan, S. A., T. G. Levitskaia, A. M. Johnsen, C. R. Orton, and J. M. Peterson. 2011. "Spectroscopic monitoring of spent nuclear fuel reprocessing streams: an evaluation of spent fuel solutions via Raman, visible, and near-infrared spectroscopy." *Radiochimica Acta* 99 (9):563-571. doi: 10.1524/ract.2011.1865.
- Bryan, S. A., T. G. Levitskaia, S. I. Sinkov, S. N. Schlahta, and J. M. Shaver. 2006. "Raman based process monitor for continuous real-time analysis of high level radioactive waste components." *Abstracts of Papers of the American Chemical Society* 232:852-852.
- Casella, A. J., L. R. H. Ahlers, E. L. Campbell, T. G. Levitskaia, J. M. Peterson, F. N. Smith, and S. A. Bryan. 2015. "Development of Online Spectroscopic pH Monitoring for Nuclear Fuel Reprocessing Plants: Weak Acid Schemes." *Analytical Chemistry* 87 (10):5139-5147.
- Casella, Amanda, Amanda Lines, Gilbert Nelson, Job Bello, and Samuel Bryan. 2016. "MicroRaman Measurements for Nuclear Fuel Reprocessing Applications." *Procedia Chemistry* 21:466-472. doi: <https://doi.org/10.1016/j.proche.2016.10.065>.
- Clifford, A. J., H. E. Lackey, G. L. Nelson, S. A. Bryan, and A. M. Lines. 2021. "Raman Spectroscopy Coupled with Chemometric Analysis for Speciation and Quantitative Analysis of Aqueous Phosphoric Acid Systems." *Anal Chem* 93 (14):5890-5896. doi: 10.1021/acs.analchem.1c00244.
- De Beer, T., A. Burggraeve, M. Fonteyne, L. Saerens, J. P. Remon, and C. Vervaet. 2011. "Near infrared and Raman spectroscopy for the in-process monitoring of pharmaceutical production processes." *International Journal of Pharmaceutics* 417 (1-2):32-47. doi: 10.1016/j.ijpharm.2010.12.012.
- De Leersnyder, F., E. Peeters, H. Djalabi, V. Vanhoorne, B. Van Snick, K. Hong, S. Hammond, A. Y. Liu, E. Ziemons, C. Vervaet, and T. De Beer. 2018. "Development and validation of an in-line NIR spectroscopic method for continuous blend potency determination in the feed frame of a tablet press." *Journal of Pharmaceutical and Biomedical Analysis* 151:274-283. doi: 10.1016/j.jpba.2018.01.032.
- Faber, N. M., and R. Bro. 2002. "Standard error of prediction for multiway PLS 1. Background and a simulation study." *Chemometrics and Intelligent Laboratory Systems* 61 (1-2):133-149. doi: Pii S0169-7439(01)00204-0
 Doi 10.1016/S0169-7439(01)00204-0.
- Felmy, H. M., A. J. Clifford, A. S. Medina, R. M. Cox, J. M. Wilson, A. M. Lines, and S. A. Bryan. 2021. "On-Line Monitoring of Gas-Phase Molecular Iodine Using Raman and Fluorescence Spectroscopy Paired with Chemometric Analysis." *Environ Sci Technol.* doi: 10.1021/acs.est.0c06137.
- Gallagher, N. B., T. A. Blake, P. L. Gassman, J. M. Shaver, and W. Windig. 2006. "Multivariate curve resolution applied to infrared reflection measurements of soil contaminated with an organophosphorus analyte." *Applied Spectroscopy* 60 (7):713-722. doi: Doi 10.1366/00037020677887026.
- Harris, D. C. 2007. *Quantitative chemical analysis*. 7 ed. New York, NY: W.H. Freeman and Co.
- Herting, D. 2003. "Inorganic Tank Waste Speciation." 58th Northwest Regional Meeting of the American Chemical Society, Bozeman, MT, June 12-14, 2003.
- Lackey, Hope E., Gilbert L. Nelson, Amanda M. Lines, and Samuel A. Bryan. 2020. "Reimagining pH Measurement: Utilizing Raman Spectroscopy for Enhanced Accuracy

- in Phosphoric Acid Systems." *Analytical Chemistry* 92 (8):5882-5889. doi: 10.1021/acs.analchem.9b05708.
- Lines, A. M., P. Tse, H. M. Felmy, J. M. Wilson, J. Shafer, K. M. Denslow, A. N. Still, C. King, and S. A. Bryan. 2019. "Online, Real-Time Analysis of Highly Complex Processing Streams: Quantification of Analytes in Hanford Tank Sample." *Industrial & Engineering Chemistry Research* 58 (47):21194-21200. doi: 10.1021/acs.iecr.9b03636.
- Lines, Amanda M., Gabriel B. Hall, Susan Asmussen, Jarrod Allred, Sergey Sinkov, Forrest Heller, Neal Gallagher, Gregg J. Lumetta, and Samuel A. Bryan. 2020. "Sensor Fusion: Comprehensive Real-Time, On-Line Monitoring for Process Control via Visible, Near-Infrared, and Raman Spectroscopy." *ACS Sensors* 5 (8):2467-2475. doi: 10.1021/acssensors.0c00659.
- Nelson, G. L., S. E. Asmussen, A. M. Lines, A. J. Casella, D. R. Bottenus, S. B. Clark, and S. A. Bryan. 2018. "Micro-Raman Technology to Interrogate Two-Phase Extraction on a Microfluidic Device." *Analytical Chemistry* 90 (14):8345-8353. doi: 10.1021/acs.analchem.7b04330.
- Nelson, G. L., H. E. Lackey, J. M. Bello, H. M. Felmy, H. B. Bryan, F. Lamadie, S. A. Bryan, and A. M. Lines. 2021. "Enabling Microscale Processing: Combined Raman and Absorbance Spectroscopy for Microfluidic On-Line Monitoring." *Analytical Chemistry* 93 (3):1643-1651. doi: 10.1021/acs.analchem.0c04225.
- Nelson, G. L., A. M. Lines, J. M. Bello, and S. A. Bryan. 2019. "Online Monitoring of Solutions Within Microfluidic Chips: Simultaneous Raman and UV-Vis Absorption Spectroscopies." *Acs Sensors* 4 (9):2288-2295. doi: 10.1021/acssensors.9b00736.
- Schroll, C. A., A. M. Lines, W. R. Heineman, and S. A. Bryan. 2016. "Absorption spectroscopy for the quantitative prediction of lanthanide concentrations in the 3LiCl-2CsCl eutectic at 723 K." *Analytical Methods* 8 (43):7731-7738. doi: 10.1039/c6ay01520d.
- Tse, P., S. A. Bryan, N. P. Bessen, A. M. Lines, and J. C. Shafer. 2020. "Review of on-line and near real-time spectroscopic monitoring of processes relevant to nuclear material management." *Analytica Chimica Acta* 1107:1-13. doi: 10.1016/j.aca.2020.02.008.

Pacific Northwest National Laboratory

902 Battelle Boulevard
P.O. Box 999
Richland, WA 99354
1-888-375-PNNL (7665)

www.pnnl.gov